



# NO<sub>x</sub> Conversion Performance Prediction of Low-Temperature Ethanol-SCR Using Machine Learning Models

Himmet ÖZARSLAN<sup>1\*</sup>  and İhsan ULUOCAK<sup>2</sup> 

<sup>1\*</sup>Department of Mechanical Engineering, Engineering Faculty, Siirt University, 56150, Siirt, Türkiye, hozarslan@siirt.edu.tr

<sup>2</sup>Department of Mechanical Engineering, Ceyhan Engineering Faculty, Cukurova University, 01950 Adana, Türkiye, ihsanuluocak@gmail.com

**Abstract.** Mitigating global warming and reducing harmful air pollution, the effective management of NO<sub>x</sub> emissions via Selective Catalytic Reduction (SCR) systems is a major priority. For this reason, This study presents a comprehensive investigation of the NO<sub>x</sub> reduction performance of Sb-doped Ce/TiO<sub>2</sub>-Cordierite catalysts within an ethanol-selective catalytic reduction (EtOH-SCR) system, modeled through machine learning techniques. The experimental phase involved the synthesis of Ce/TiO<sub>2</sub>-Cordierite catalysts doped with different molar ratios of antimony (Sb) using the wash-coating method. Ce and Sb acted as active components, TiO<sub>2</sub> served as the secondary support, and cordierite functioned as the primary carrier material. Performance evaluations under real engine exhaust conditions revealed that Sb incorporation remarkably improved low-temperature catalytic activity. The maximum NO<sub>x</sub> conversion efficiency reached 93.24% at 270 °C, 40,000 h<sup>-1</sup> space velocity, and 5 kW engine load for the 1.33SCT catalyst. To further predict and analyze system behavior under varying temperature and load conditions, SVM and Ensemble of Trees models were developed. The proposed framework integrates experimental insights with data-driven modeling to enhance the understanding and optimization of low-temperature SCR systems for cleaner engine applications.

**Keywords:** NO<sub>x</sub> reduction, SCR, Optimization, Machine learning.

## 1. Introduction

Diesel engines continue to be widely used due to their high efficiency and durability; however, the resulting nitrogen oxide (NO<sub>x</sub>) emissions remain a major environmental and regulatory challenge. Selective Catalytic Reduction (SCR) is one of the most effective methods for NO<sub>x</sub> removal, yet conventional NH<sub>3</sub>-SCR suffers from limitations such as ammonia slip, crystallization issues, and poor low-temperature performance [1]. As a result, ethanol-SCR has gained increasing interest, with ethanol proven to be an efficient reductant over various silver- and oxide-based catalysts [1]. Catalyst for-

mulation plays a critical role, and cerium (Ce) has been shown to enhance oxygen storage capacity, redox behavior, and surface acidity, improving NO<sub>x</sub> conversion and stability in SCR systems [1–3].

Recent studies also reveal that antimony (Sb) acts as an effective promoter by increasing surface acidity, stabilizing oxygen vacancies, and enhancing NO and hydrocarbon adsorption, which benefits both L–H and E–R reaction pathways [4]. In addition, Sb prevents calcium poisoning and maintains ethanol activation routes, contributing to improved NO<sub>x</sub> reduction under real exhaust conditions [5]. Sb modification of Ce-based catalysts has further demonstrated higher NO<sub>x</sub> conversion and N<sub>2</sub> selectivity across wide temperature ranges [6]. Despite these advances, the combined effect of Ce and Sb in ethanol-SCR under real diesel exhaust remains insufficiently studied, especially at low temperatures and varying engine loads.

However, optimizing SCR systems solely through experimental methods is time-consuming and resource-intensive due to the complex, non-linear interactions between operating parameters such as temperature, space velocity, and engine load. To address this, data-driven approaches, particularly Machine Learning (ML) algorithms, have emerged as powerful tools for modeling catalytic behaviors. Integrating advanced models, such as Support Vector Machines (SVM) and Ensemble of Trees, with experimental data allows for a precise prediction of NO<sub>x</sub> conversion efficiency, offering a cost-effective pathway to understand system dynamics without extensive physical testing.

This study evaluates Ce- and Sb-modified catalysts for ethanol-SCR using real diesel engine exhaust at 190–270 °C and 1–3–5 kW engine loads. The objective is not only to determine the low-temperature NO<sub>x</sub> conversion behavior and the influence of Ce/Sb incorporation but also to develop and validate robust machine learning models capable of predicting the system's performance under realistic operating conditions.

## 2. Material and Method

### 2.1. Catalyst Preparation

A commercially available cordierite monolith (2Al<sub>2</sub>O<sub>3</sub>–5SiO<sub>2</sub>–2MgO) with a cell density of 400 cpsi was employed as the structural substrate for catalyst fabrication. To synthesize the powdered catalyst, a solution containing 0.015 mol of cerium (III) acetate hydrate (Ce(CH<sub>3</sub>CO<sub>2</sub>)<sub>3</sub>·xH<sub>2</sub>O) as the cerium precursor and 0.3 mol of TiO<sub>2</sub> dispersed in 150 mL of deionized water was magnetically stirred until complete evaporation of water. The resulting mixture was dried in an oven at 120 °C for 3 h, followed by calcination at 550 °C for 3 h in a muffle furnace. The calcined material was then ground into a fine powder. All powdered catalysts were synthesized following the same procedure.

For coating preparation, the obtained catalyst powder was dispersed in 300 mL of deionized water together with 3 g of Ludox HS-40 colloidal silica as a binding agent. The mixture was stirred for 1 h to ensure homogeneity. Acid-treated cordierite substrates were then immersed in this slurry and dried at 140 °C for 1 h. This impregnation and drying cycle was repeated three times to achieve uniform coating. Subsequently,

the coated cordierite samples were calcined at 550 °C for 3 h in a muffle furnace to obtain the final catalysts.

The Ce/Ti molar ratio was fixed at 0.05 for all prepared samples. Antimony(III) oxide ( $\text{Sb}_2\text{O}_3$ ), supplied by Across Company, was used as the antimony source in the doped catalysts, while all other reagents were purchased from Sigma-Aldrich. A series of Sb-Ce/TiO<sub>2</sub>/cordierite catalysts with varying Sb contents were prepared and designated as  $\rho$ -Sb-Ce/TiO<sub>2</sub>/Cor, where  $\rho$  represents the Sb/Ce molar ratio. Accordingly, catalysts with ratios of 0.66 and 1.33 were named 0.66-Sb-Ce/TiO<sub>2</sub>/Cor and 1.33-Sb-Ce/TiO<sub>2</sub>/Cor, respectively. Additional samples were synthesized following the same protocol, with compositions listed in Table 1. Based on their compositions, the catalysts were labeled as follows: CT (Ce/TiO<sub>2</sub>/Cor), 0.66-SCT (0.66-Sb-Ce/TiO<sub>2</sub>/Cor), and 1.33-SCT (1.33-Sb-Ce/TiO<sub>2</sub>/Cor).

**Table 1.** Rate of compositions of the prepared catalysts

Catalysts	Abbr. of Catalysts	Molar amounts			
		Ce(CH <sub>3</sub> CO <sub>2</sub> ) <sub>3</sub> .xH <sub>2</sub> O (mol)	Sb <sub>2</sub> O <sub>3</sub> (mol)	TiO <sub>2</sub> (mol)	Molar ratio
Ce/TiO <sub>2</sub> /Cor	CT	0.015	-	0.3	Ce/Ti = 0.05
0.66-Sb-Ce/TiO <sub>2</sub> /Cor	0.66-SCT	0.015	0.01	0.3	Sb/Ce = 0.66
1.33-Sb-Ce/TiO <sub>2</sub> /Cor	1.33-SCT	0.015	0.02	0.3	Sb/Ce = 1.33

## 2.2. Experimental Setup

The experimental investigations were conducted on an AKSA A2CRX08 diesel engine configured with two cylinders and operating at a constant speed of 3000 rpm. The engine features a bore of 80 mm and a stroke of 79 mm, yielding a total displacement of 830 cm<sup>3</sup> and a compression ratio of 23:1. A water-cooled thermal management system was employed to maintain steady operating temperatures during prolonged testing under various load conditions.

For exhaust emission control, the setup incorporated a post-treatment unit consisting of a load control system, a microprocessor module, an exhaust gas heater, a selective catalytic reduction (SCR) reactor, and a diesel oxidation catalyst (DOC). Ethanol was used as the reducing agent and supplied via a six-hole electro-hydraulic injector driven by an electric fuel pump. The injector was positioned in a dedicated mixing chamber located between the DOC and SCR units. Exhaust gas flow was measured using an orifice plate, and corresponding pressure values were recorded through a U-tube manometer. The space velocity (SV, h<sup>-1</sup>) was defined as the ratio of the hourly volumetric exhaust flow rate (V<sub>f</sub>, m<sup>3</sup>/h) to the catalyst volume (V<sub>c</sub>, m<sup>3</sup>) [7].

Engine loading was achieved through a resistive heating assembly composed of multiple 1 kW heater elements, which allowed the applied load to be increased in 1 kW increments. By selectively engaging these elements, the desired load levels were imposed in a controlled and repeatable manner. This configuration enabled systematic

variation of engine operating conditions while maintaining stable thermal characteristics, ensuring consistent evaluation of catalyst performance at each load stage.

Exhaust temperature regulation was achieved using K-type thermocouples with an operating range of  $-200$  to  $1370$  °C. The thermocouples provided real-time feedback to an electric heater that maintained the exhaust gas temperature between  $190$  °C and  $270$  °C during the tests. Flow control valves and an orifice plate were used to establish a constant space velocity of approximately  $40,000$  h<sup>-1</sup> before passing through the DOC and entering the reductant injection zone.

Emission measurements were performed using two Continental UniNO<sub>x</sub> sensors positioned upstream and downstream of the SCR unit to determine NO<sub>x</sub> concentrations at the inlet and outlet. These sensors operate over a detection range of  $0$ – $1500$  ppm with an accuracy of  $\pm 1.5\%$ . Continuous real-time monitoring of NO<sub>x</sub> levels and exhaust temperature was accomplished through a digital data interface. Sensor signals were transmitted to a data acquisition platform via a CANBUS Shield connected to an Arduino Due microcontroller, enabling synchronized recording of exhaust gas composition. The ethanol delivery system employed an SRD-05VDC-SL-C controlled electric pump that maintained a stable pressure of  $3$ – $3.5$  bar to the six-hole injector. This regulated pressure ensured efficient atomization and homogeneous mixing of ethanol with the exhaust stream, optimizing the reduction process.

The NO<sub>x</sub> conversion efficiency (%) was calculated according to Eq. (1):

$$\text{NO}_x \text{ Conversion (\%)} = \left( \frac{[\text{NO}_x]_{\text{in}} - [\text{NO}_x]_{\text{out}}}{[\text{NO}_x]_{\text{in}}} \right) \times 100 \quad (1)$$

All experiments were conducted under standardized and repeatable conditions. Before each test, the engine was preheated for approximately 30 minutes to achieve thermal equilibrium. Each catalyst configuration was evaluated at a fixed space velocity of  $40,000$  h<sup>-1</sup> over the  $190$ – $270$  °C temperature range. The effect of engine load on catalytic performance was examined at three discrete levels:  $1$  kW,  $3$  kW, and  $5$  kW. Load adjustments were performed in  $1$  kW increments through selective activation of the resistive heaters, allowing precise control of mechanical output. This procedure ensured stable exhaust temperature and flow characteristics, providing a consistent and reliable framework for assessing NO<sub>x</sub> conversion efficiency under varying operating conditions.

## 2.3. Prediction Models

### 2.3.1. Support Vector Machine (SVM)

The SVM algorithm is a supervised learning technique based on the principle of structural risk minimization [8]. For regression tasks (SVR), the algorithm seeks to define a function that deviates from the actual target values by a value no greater than a specified margin (epsilon) while keeping the model weights as flat as possible. To handle the non-linear nature of the SCR catalytic process, a kernel function (specifically the Gaussian kernel) was utilized to map the input data into a higher-dimensional feature space, enabling the separation of complex patterns.

### 2.3.2. Ensemble of Trees

The Ensemble of Trees method improves predictive accuracy by aggregating the results of multiple weak learners (decision trees) to form a single strong learner [9]. In this study, the LSBoost (Least Squares Boosting) algorithm was selected. LSBoost sequentially fits regression trees to the residuals of the previous trees, effectively minimizing the mean squared error at each step. This approach is particularly robust against overfitting and is highly effective for datasets with non-linear characteristics.

### 2.3.3. Hyperparameter Optimization and Validation Strategy

To ensure optimal model performance, Bayesian Optimization was applied for hyperparameter tuning. Unlike traditional grid search or random search methods, Bayesian Optimization constructs a probabilistic model of the objective function and iteratively selects hyperparameters to evaluate, thereby efficiently converging to the global minimum of the validation error with 30 iterations. To assess the statistical reliability and generalization capability of the models, a 5-fold cross-validation technique was employed. The dataset was randomly partitioned into five equal subsets (folds). The model was trained on four folds and validated on the remaining fold, with this process repeated five times. The final performance was evaluated using key statistical metrics with 20 % of the whole dataset: Coefficient of Determination ( $R^2$ ), Root Mean Squared Error (RMSE), and Mean Absolute Error (MAE).

## 3. Results and Discussion

### 3.1. NO<sub>x</sub> conversion rates

Figure 1 illustrates the effect of reaction temperature on NO<sub>x</sub> conversion efficiency at different engine load conditions. As the temperature increased from 190 °C to 270 °C in 10 °C increments, a continuous improvement in NO<sub>x</sub> conversion was evident under all operational loads, demonstrating a strong temperature-dependent enhancement in catalytic activity. The results further reveal that elevating the engine load from 1 kW to 5 kW contributed to additional increases in conversion efficiency, indicating that higher power demand promotes more favorable reaction conditions. Overall, the combination of increased temperature and engine load (evaluated under a space velocity of 40,000 h<sup>-1</sup>) significantly boosted NO<sub>x</sub> reduction performance. The maximum conversion values were consistently obtained at 270 °C for all load levels, confirming this temperature as the optimum operating point for the catalyst.

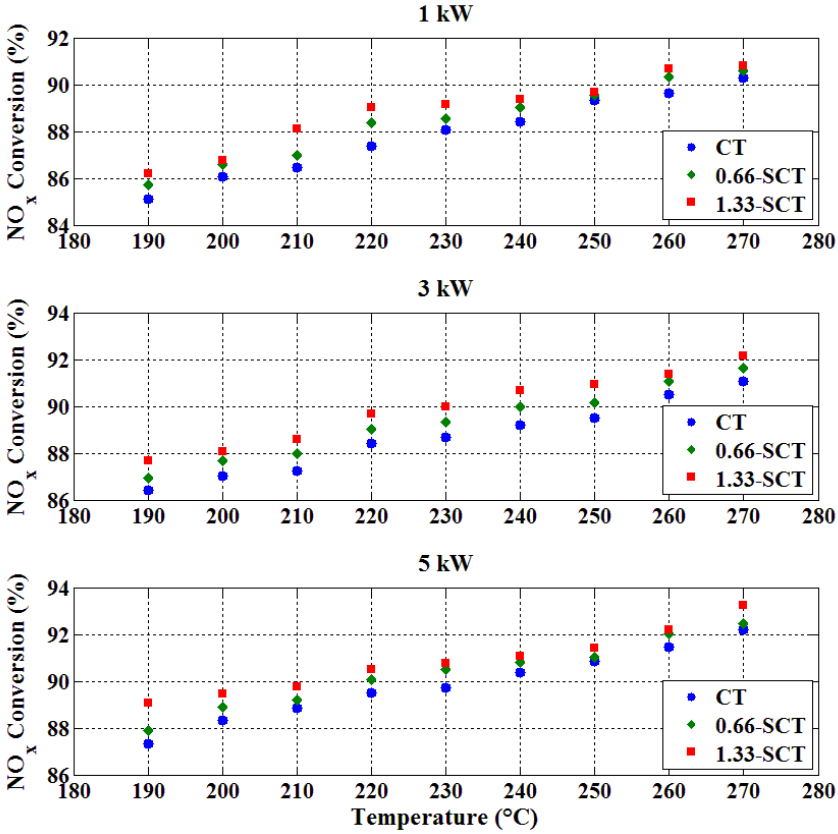


**Fig. 1.** NO<sub>x</sub> Conversion rates of Sb-Ce containing catalysts under 1-3-5 kW engine loads

The maximum NO<sub>x</sub> conversion efficiencies were determined as 93.24%, 92.46%, and 92.20% for the 1.33-SCT, 0.66-SCT, and CT catalysts, respectively, at 270 °C under a 5 kW engine load. Across all operating conditions, the lowest conversion value was observed for the CT catalyst, which achieved only 85.11% NO<sub>x</sub> reduction at 190 °C and 1 kW. Conversely, the highest performance (93.24%) was obtained with the 1.33-SCT catalyst at 270 °C and 5 kW, demonstrating its superior activity among the synthesized catalyst formulations.

The evaluation of the three catalyst samples (CT, 0.66-SCT, and 1.33-SCT) demonstrated a clear enhancement in NO<sub>x</sub> conversion efficiency with increasing exhaust temperature. This improvement in catalytic performance up to 270 °C confirms the strong temperature dependence of the ethanol-SCR process and is consistent with trends previously documented in the literature [10-12].

Figure 1 further illustrates the influence of engine load on catalyst behavior at 1, 3, and 5 kW. A modest but noticeable increase in NO<sub>x</sub> conversion was observed as the load increased. This enhancement is attributed to the greater availability of hydrocarbon radicals at higher loads, which facilitates the reduction of NO<sub>2</sub> to N<sub>2</sub>, CO<sub>2</sub>, and H<sub>2</sub>O

within the HC-SCR mechanism. The enriched mixture conditions associated with elevated load levels also contribute to changes in exhaust composition, thereby promoting more efficient catalytic reactions [13, 14].

### 3.2. Modelling Procedure

Building upon the experimental findings, this section focuses on the development and validation of data-driven models to predict the NO<sub>x</sub> conversion efficiency of the optimized EtOH-SCR system. Given the complex and non-linear relationship between engine operating parameters (temperature, load) and catalytic performance, Support Vector Machine (SVM) and Ensemble of Trees (using LSBoost) algorithms were employed to capture system behavior. To ensure the development of robust and generalized models, the experimental dataset was subjected to rigorous preprocessing and partitioning.

A critical aspect of the modeling strategy involved the use of Bayesian Optimization for hyperparameter tuning. Unlike traditional grid search methods, Bayesian Optimization was utilized to efficiently navigate the hyperparameter space, minimizing the objective function to enhance prediction accuracy. Furthermore, to assess the statistical reliability of the models and mitigate the risk of overfitting, a 5-fold cross-validation scheme was implemented. The following subsections present a detailed comparative analysis of the developed models, evaluated through statistical metrics and graphical parity plots to demonstrate their predictive capabilities under varying engine conditions.

For the Support Vector Machine (SVM) model, a Gaussian kernel function was selected to handle the non-linear nature of the dataset. The optimization process converged at a box constraint of 5.5312 and an epsilon value of 0.0026. The box constraint controls the penalty for misclassification, while epsilon determines the margin of tolerance for errors; these specific values suggest a model configured to capture fine-grained patterns in the NO<sub>x</sub> conversion data without succumbing to overfitting.

Regarding the Ensemble of Trees model, the optimization yielded a compact structure. The model was tuned to a minimum leaf size of 1, utilizing 10 learners (decision trees) with a learning rate of 0.796. The relatively high learning rate combined with a specific number of learners indicates that the boosting algorithm rapidly converged to an optimal solution, effectively correcting the residual errors of preceding trees.

The predictive accuracy of the developed models was quantitatively evaluated using standard statistical metrics, as summarized in Table 2. Both algorithms demonstrated high precision in capturing the non-linear NO<sub>x</sub> conversion behavior, with coefficient of determination ( $R^2$ ) values exceeding 0.96. Comparative analysis reveals that the SVM model yielded slightly superior overall performance, achieving the highest  $R^2$  of 0.969 and the lowest RMSE of 0.315, which indicates a robust fit with minimal large error deviations. Although the Ensemble of Trees model exhibited a marginally lower MAE (0.264), the SVM's lower MSE (0.098) and higher correlation confirm its suitability as the primary model for predicting system performance under the investigated operating conditions.

**Table 2.** Accuracy Metrics Results

Model Type	MAE	RMSE	R <sup>2</sup>
Ensemble of Trees	0.264	0.331	0.965
SVM	0.284	0.315	0.969

Figure 2 visually represent the performance of the Ensemble of Trees and SVM models, respectively, by comparing their predicted NO<sub>x</sub> conversion values against the actual experimental observations. In both figures, the solid diagonal line signifies perfect prediction, where all predicted values would exactly match the true responses. Generally, both models demonstrated strong predictive capabilities, with most data points closely aligned with this perfect prediction line. Although some minor scattering of data points is observable, particularly for the Ensemble of Trees model, the overall trend confirms that the predictions for both algorithms are notably close to the experimental reality.

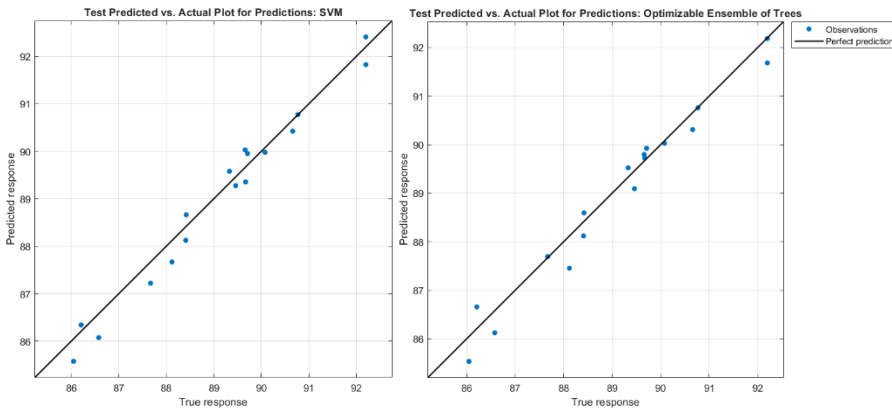


**Fig. 2.** Regression graphs for the offered models

To rigorously investigate the error characteristics of the developed models, residual plots were generated and are presented in Figure 3. These plots illustrate the difference between the predicted and actual NO<sub>x</sub> conversion values (residuals) across the test dataset. A robust model is characterized by a random distribution of residuals around the horizontal zero line, indicating the absence of systematic bias or non-linear patterns missed by the model. As observed in the figures, both models exhibit a generally stochastic distribution of residuals centered around zero, which confirms that the assumption of independent and identically distributed errors holds true. However, a closer inspection reveals a distinction in the magnitude of deviations. The Ensemble of Trees model displays several residuals with larger magnitudes (exceeding 0.6 %), suggesting

occasional outliers in prediction. In contrast, the SVM model demonstrates a more confined residual spread, with the majority of error values remaining within a narrower range (0.5 %). This tighter clustering of residuals around the zero axis further corroborates the previously discussed statistical metrics, reinforcing the conclusion that the SVM algorithm offers slightly superior stability and precision in predicting the catalytic performance.

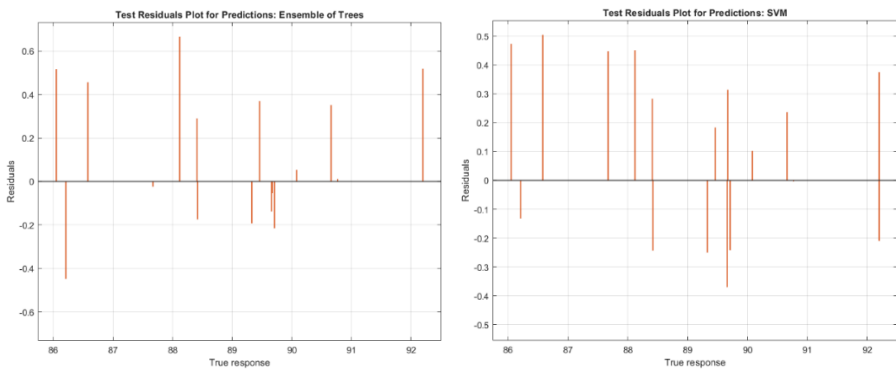


**Fig. 3.** Residual Graph for SVM and Ensemble of Trees

## 4. Conclusion

This study successfully integrated experimental analysis with advanced machine learning to optimize the NO<sub>x</sub> reduction performance of Sb-doped Ce/TiO<sub>2</sub>-Cordierite catalysts for EtOH-SCR systems. Experimental results identified the 1.33SCT catalyst as the optimal formulation, achieving a peak NO<sub>x</sub> conversion efficiency of 93.24% at 270 °C under real engine conditions. To model this non-linear system, Ensemble of Trees and Support Vector Machine (SVM) algorithms were developed using Bayesian Optimization and 5-fold cross-validation. While both models exhibited strong predictive capabilities, the SVM algorithm demonstrated superior accuracy and robustness, achieving the highest coefficient of determination ( $R^2 = 0.969$ ) and the lowest RMSE (0.315). Visual validation through parity and residual plots further confirmed the SVM's stability in minimizing systematic errors. Ultimately, this work establishes that combining high-performance catalysts with data-driven SVM modeling provides a reliable, cost-effective framework for the design and optimization of next-generation low-temperature emission control technologies.

Furthermore, future research should explore hybrid deep learning architectures to capture dynamic temporal dependencies in transient engine cycles, potentially offering even greater predictive precision

## References

1. Ozarslan, H., Keskin, A. & Resitoglu, I.A. Enhancing low-temperature ethanol-selective catalytic reduction over Ag/TiO<sub>2</sub>-cordierite catalysts via cerium addition. *Reac Kinet Mech Cat* 138, 2351–2368 (2025). <https://doi.org/10.1007/s11144-025-02855-7>
2. Pang L., Fan C., Shao L., Song K., Yi J., Cai X. Wang J., Kang M., Li T., The Ce-doping Cu/ZSM-5 as a new superior catalyst to remove NO from diesel engine exhaust. *Chemical Engineering Journal*, 2014; 253: 394-401. <https://doi.org/10.1016/j.cej.2014.05.090>
3. Zhang Y., Zhao L., Duan J., Bi S. Insights into deNO<sub>x</sub> processing over Ce-modified Cu-BTC catalysts for the CO-SCR reaction at low temperature. *Separation and Purification Technology*, 2020;234: 116081. <https://doi.org/10.1016/j.seppur.2019.116081>
4. Wang Z., Guo R., Shi X., Pan W., Liu J., Sun X., Liu S., Liu X., Qin H. The enhanced performance of Sb-modified Cu/TiO<sub>2</sub> catalysts for selective catalytic reduction of NO<sub>x</sub> with NH<sub>3</sub>, 2019;475: 334-341. <https://doi.org/10.1016/j.apsusc.2018.12.281>
5. Resitoglu, I.A.; Keskin, A.; Karaman, B.; Ozarslan, H. Suppressing Calcium Deactivation in Selective Catalytic Reduction of NO<sub>x</sub> from Diesel Engines Using Antimony. *Processes* 2025, 13, 1914. <https://doi.org/10.3390/pr13061914>
6. Wu G., Guo R., Liu Y., Duan C., Miao Y., Gu J., Pan W. Promoting effect of Sb on the selective catalytic reduction of NO with NH<sub>3</sub> over CeVO<sub>4</sub> catalyst. *Journal of the Energy Institute*, 2021;95: 77-86. <https://doi.org/10.1016/j.joei.2021.01.003>
7. Reşitoglu IA, Altinişik K, Keskin A. The pollutant emissions from diesel-engine vehicles and exhaust aftertreatment systems. *Clean Techn Environ Policy* 2015;17: 15–27. <https://doi.org/10.1007/s10098-014-0793-9>.
8. Uluocak, Ihsan, and Erinc Uludamar. "Comparative evaluation of machine learning models for predicting noise and vibration of a biodiesel-CNG fuelled diesel engine." *Measurement* 249 (2025): 117021. <https://doi.org/10.1016/j.measurement.2025.117021>
9. Uludamar, Erinc, and Ihsan Uluocak. "Artificial Intelligence-Based prediction of engine noise and vibration in Biodiesel-Diesel engines with hydrogen injection." *Fuel* 385 (2025): 134071. <https://doi.org/10.1016/j.fuel.2024.134071>
10. Gunnarsson F, Kannisto H, Skoglundh M, Harelind H. Improved low-temperature activity of silver-alumina for lean NO<sub>x</sub> reduction-effects of Ag loading and low level Pt doping. *Appl Catal B* 2014;152–153:218–25. <https://doi.org/10.1016/j.apcatb.2014.01.043>.
11. Lee, K.; Choi, B.; Kim, C.; Lee, C.; Oh, K. De-NO<sub>x</sub> characteristics of HC-SCR system employing combined Ag/Al<sub>2</sub>O<sub>3</sub> and CuSn/ZSM-5 catalyst. *J. Ind. Eng. Chem.* 2021, 93, 461–475. <https://doi.org/10.1016/j.jiec.2020.10.026>
12. Khatrı, P.; Bhatia, D. Influence of catalyst composition on NO<sub>x</sub> storage and reduction characteristics of Ag catalyst supported on MgO-doped alumina. *Chem. Eng. Res. Des.* 2023, 197, 476–495. <https://doi.org/10.1016/j.cherd.2023.07.044>
13. Bai, S.; Han, J.; Liu, M.; Qin, S.; Wang, G.; Li, G. Experimental investigation of exhaust thermal management on NO<sub>x</sub> emissions of heavy-duty diesel engine under the world Harmonized transient cycle (WHTC). *Appl. Therm. Eng.* 2018, 142, 421–432. <https://doi.org/10.1016/j.applthermaleng.2018.07.042>
14. Boriboonsomsin, K.; Durbin, T.; Scora, G.; Johnson, K.; Sandez, D.; Vu, A.; Jiang, Y.; Burnette, A.; Yoon, S.; Collins, J.; et al. Real-world exhaust temperature profiles of on-road heavy-duty diesel vehicles equipped with selective catalytic reduction. *Sci. Total Environ.* 2018, 634, 909–921. <https://doi.org/10.1016/j.scitotenv.2018.03.362>

**Open Access** This chapter is licensed under the terms of the Creative Commons Attribution-NonCommercial 4.0 International License (<http://creativecommons.org/licenses/by-nc/4.0/>), which permits any noncommercial use, sharing, adaptation, distribution and reproduction in any medium or format, as long as you give appropriate credit to the original author(s) and the source, provide a link to the Creative Commons license and indicate if changes were made.

The images or other third party material in this chapter are included in the chapter's Creative Commons license, unless indicated otherwise in a credit line to the material. If material is not included in the chapter's Creative Commons license and your intended use is not permitted by statutory regulation or exceeds the permitted use, you will need to obtain permission directly from the copyright holder.

